I-SUPPORTING METHODS AND FIGURES

Using distal site mutations and allosteric inhibition to tune, extend and narrow the useful dynamic range of aptamer-based sensors

Alessandro Porchetta[1, 2, 7], Alexis Vallée-Bélisle[3, 4, 6, 7], Kevin W. Plaxco[3, 4, 5], Francesco Ricci[1, 2, *]

[1] Dipartimento di Scienze e Tecnologie Chimiche, University of Rome, Tor Vergata, Via della Ricerca Scientifica, 00133, Rome, Italy, [2] Consorzio Interuniversitario Biostrutture e Biosistemi "INBB", Rome, Italy, [3] Department of Chemistry and Biochemistry, [4] Center for Bioengineering, [5] Interdepartmental Program in Biomolecular Science and Engineering, University of California, Santa Barbara, CA 93106 USA; [6] Laboratory of Biosensors & Nanomachines, Département de Chimie, Université de Montréal, C.P. 6128, Succursale Centre-ville, Montréal, Québec H3C 3J7, Canada. [7] These authors contributed equally to this work.
*Corresponding author:francesco.ricci@uniroma2.it

All experiments were conducted at pH 7.0 in 50 mM sodium phosphate buffer at 25 °C. All fluorescence measurements were obtained using a Cary Eclipse Fluorimeter (Varian) with excitation at 480 (±5) nm and acquisition between 510 and 520 nm using 5 nm bandwidths. The fluorescence of the open state was set relative to 1 for all normalized figures. Binding curves were obtained using 100 nM aptamer beacon by sequentially increasing the target concentration via the addition of small volumes of solutions with increasing concentration of cocaine and the same aptamer concentration. For studies employing allosteric inhibitors we incubated the aptamer with the relevant inhibitor for 15 minute prior to adding the cocaine target.

The observed K_d were obtained using Eq.1:

$$F(T) = F(0) + \left(\frac{[T] * (F_B - F_0)}{[T] + K_d^{obs}} \right) \quad \text{(Eq.1)}$$

Extended binding curves were obtained following two different strategies. In the first strategy (Figure S4) we used different variants of aptamer at the optimal mixtures predicted by our

simulations [Vallée-Bélisle *et al*., 2012] and a total aptamer concentration of 100 nM. In a second strategy (Figure 4) we used our *parent* aptamer (125 nM) in a mixture containing two different inhibitors (inhibit_10, 44 nM and inhibit_14, 56 nM). Binding curves obtained with these two strategies were fitted to a log-linear function of target concentration.

Narrowed dynamic range sensors (Figure 5) were obtained using solutions of 100 nM low-affinity (but signalling-competent) aptamer (variant 2, K_d= 82.1 μM, Figure S5) together with a high-affinity (but non-signalling) variant (unlabeled parent, K_d= 4 μM. Figure S5). The resulting data were fitted to the Hill equation, which is used to describe ultrasensitive systems in biochemistry (*n* = Hill coefficient) (Eq. 2) [Hill, 1910].

$$F(T) = F(0) + \left(\frac{[T]^n * (F_B - F_0)}{[T]^n + K_d{}^{obs}} \right) \quad \text{(Eq.2)}$$

Materials and methods

HPLC-purified cocaine aptamers modified with a 5'-FAM and a 3'-BHQ-1 or (3'-DABCYL) were purchased from by BioSearch, Tech (Novato, CA). All reagent-grade chemicals, including potassium phosphate monobasic, dibasic and cocaine (all from Sigma-Aldrich, St. Louis, Missouri) were used without further purification. The aptamer sequences are reported below:

***Parent aptamer*:** 5'(FAM)-GGG AGA CAA GGA AAA TCC TTC AAT GAA GTG GGT CGA CA(BHQ)-3'

Variant 1: 5'(FAM)-ATC CTT CAA TGA AGT GGG TCG AAA GGA GAC AAG GAT (DABCYL)-3'

Variant 2: 5'(FAM)-C CTT CAA TGA AGT GGG TCG AAA GGA GAC AAG G (DABCYL) 3'

Variant 3: 5'(FAM)-GAC AAG GAG AAT CCT TCA TTG AAG TGG GTC(DABCYL)-3'

Mut_1: 5'(FAM)-AA CAA GGA AAA TCC TTC AAT GAA GTG GGT T-(DABCYL)-3'

Mut_2: 5'(FAM)-GA CAA GGA AAA TCC TTC AAT GAA GTG GGT T-(DABCYL)-3'

Mut_3: 5'(FAM)-GA CAA GGA AAA TCC TTC AGT GAA GTG GGT C-(DABCYL)-3'

Mut_4: 5'(FAM)-GA CAA GGA AAA TTC TTC AAT GAA GTG GGT C-(DABCYL)-3'

The unlabelled oligonucleotide DNAs employed in this work were synthesized and purified by Sigma-Aldrich and used as received. They were used like inhibitors of the parent aptamer (Figure 3) and as depletant in solution (Figure 5). There sequences are as follows:

Inhib_10: 5'-CTT GTC TCC C-3'
Inhib_11: 5'-CCT TGT CTC CC-3'
Inhib_12: 5'-TCC TTG TCT CCC-3'
Inhib_13: 5'-TTC CTT GTC TCC C-3'
Inhib_14: 5'-TTT CCT TGT CTC CC-3'
Inhib_15: 5'-TTT TCC TTG TCT CCC-3'
Depletant: 5'-GGG AGA CAA GGA AAA TCC TTC AAT GAA GTG GGT CGA CA-3'

Bibliography:

Hill, A. V. *J Physiol* **1910**, *40*: iv-vii.

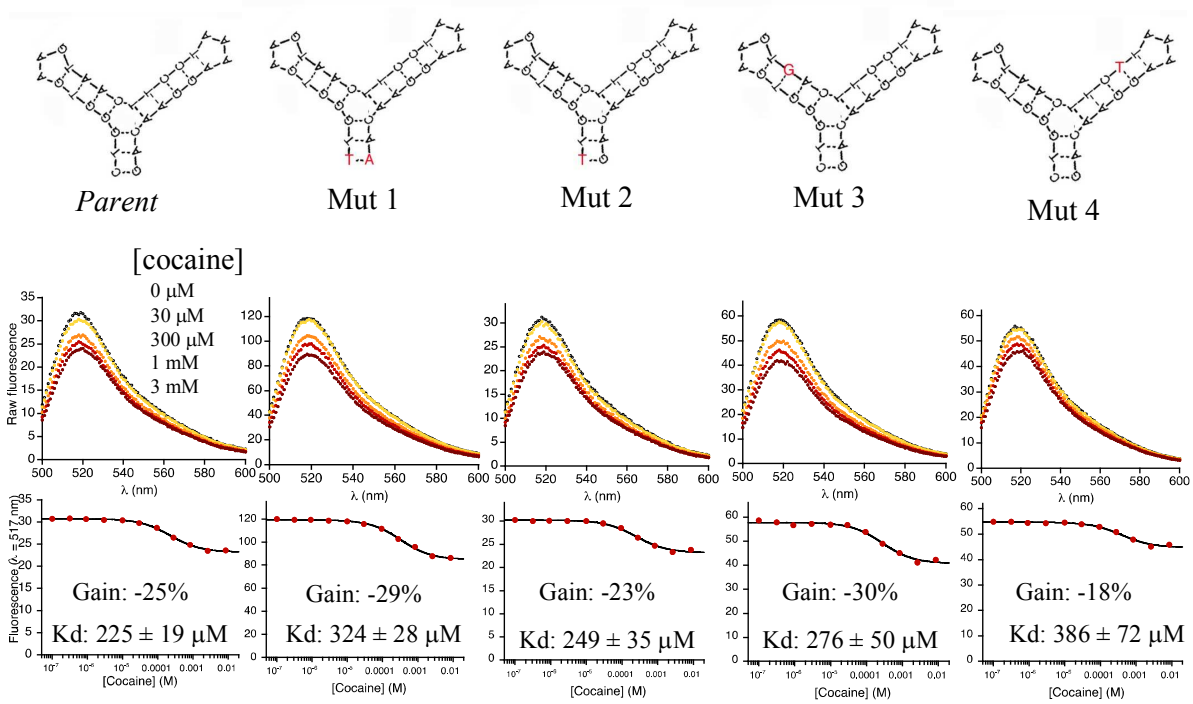

Figure S1: Tuning affinity of an aptamer via point mutation: We generated a number of variant cocaine aptamers via point mutation of the parent aptamer sequence. Our success in using this approach to generate altered affinity variants, however, was almost non-existent.

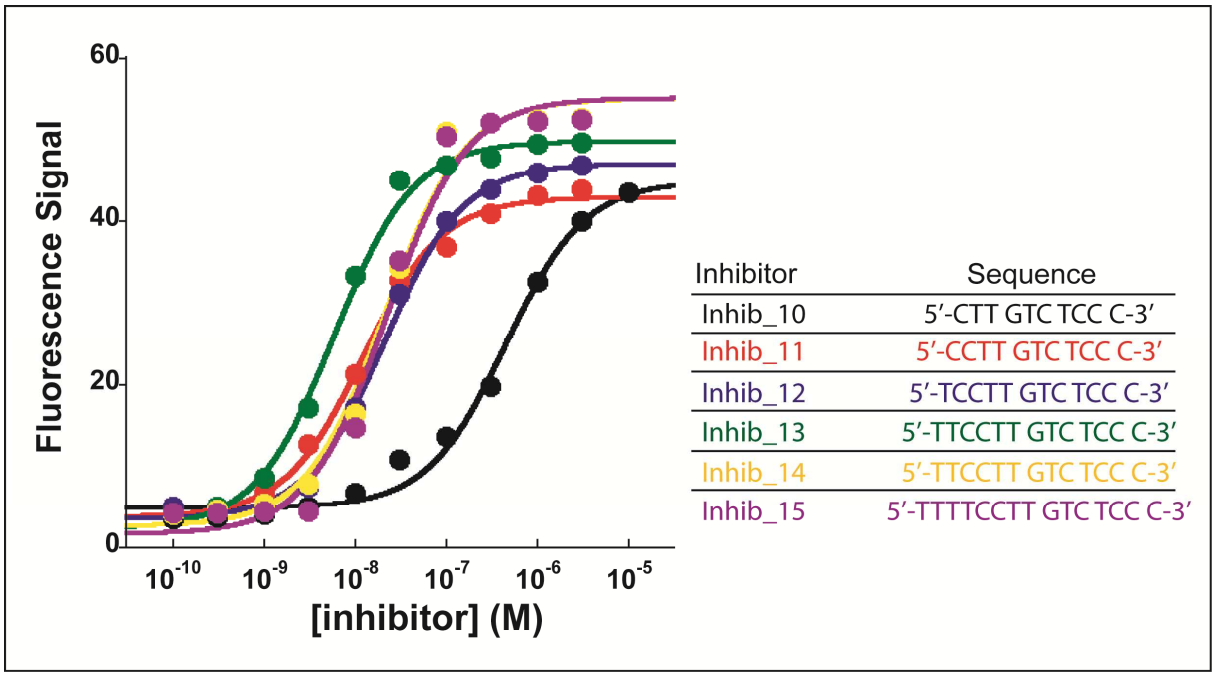

Figure S2: Oligonucleotides that specifically bind to a portion of the parent cocaine aptamer stabilize non-cocaine-binding conformations and thus act as allosteric inhibitors. Here we explored the inhibition properties of inhibitors varying in length from 10 to 15 bases. Inhibitor binding "opens" the structure of the aptamer, causing a concomitant signal change that can be used to evaluate the inhibitor's affinity for the aptamer.

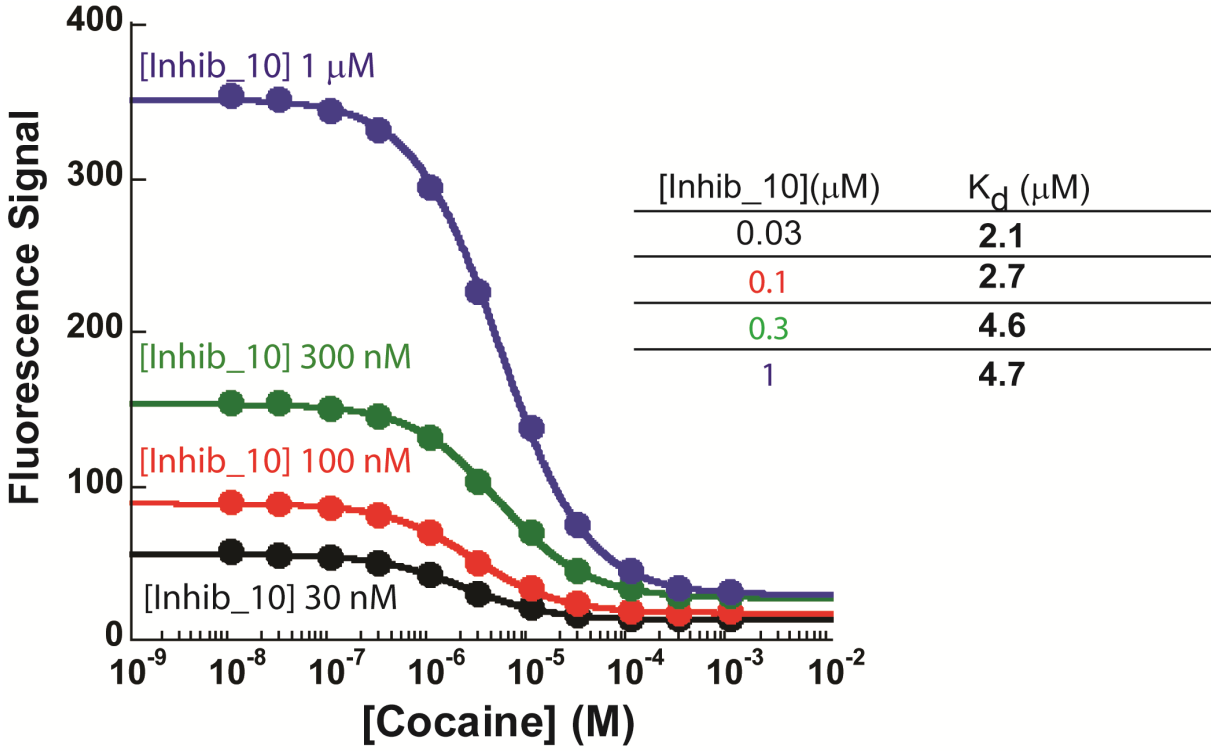

Figure S3: We can finely tune the affinity of an allosterically-inhibited aptamer by varying the inhibitor concentration. Here we have used the parent aptamer at a concentration of 100 nM and different concentrations of the 10mer allosteric inhibitor inhibit_10. Together with a fine modulation of the observed affinity (K_d) we also observe a change in the total signal gain of the sensor because inhibitor binding leads to a larger population of the probe in the open non-signaling conformation and thus to a larger signal change in presence of target (see Figure 3 for inhibition mechanism) .

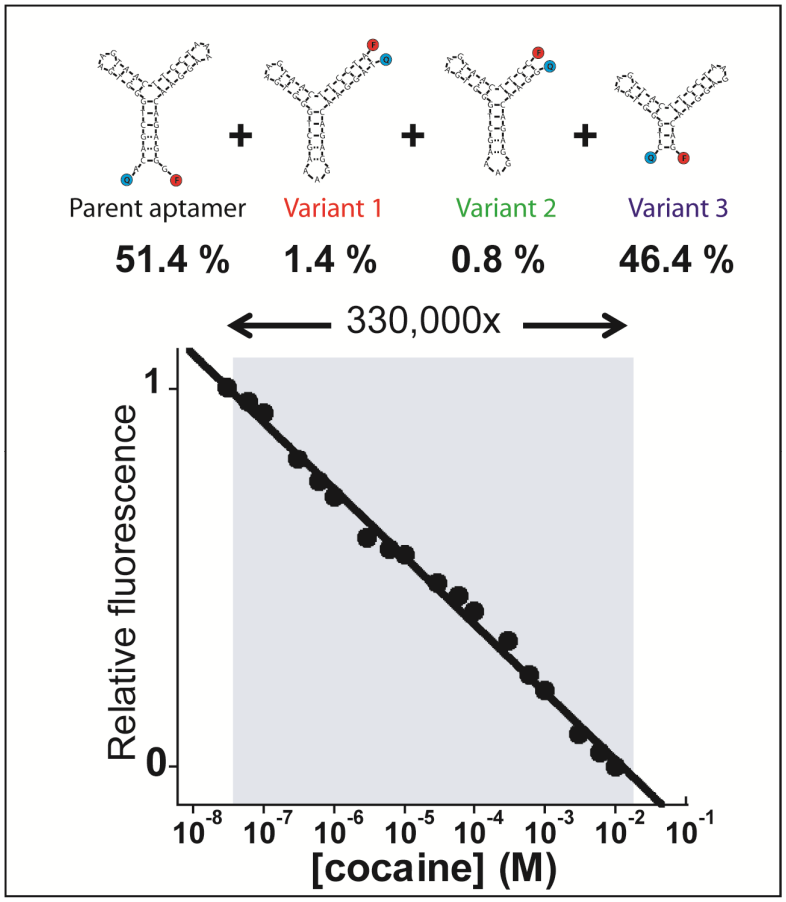

Figure S4: Extending the dynamic range using a mixture of variants: We have extended the useful 81-fold dynamic range of our model sensor to 330,000-fold by combining (in one test tube) four aptamer variants (the parent aptamer and three distal site mutants) with affinities varying across ~3 orders of magnitude. See SI text for details on how the relative concentrations of the variants were optimized.

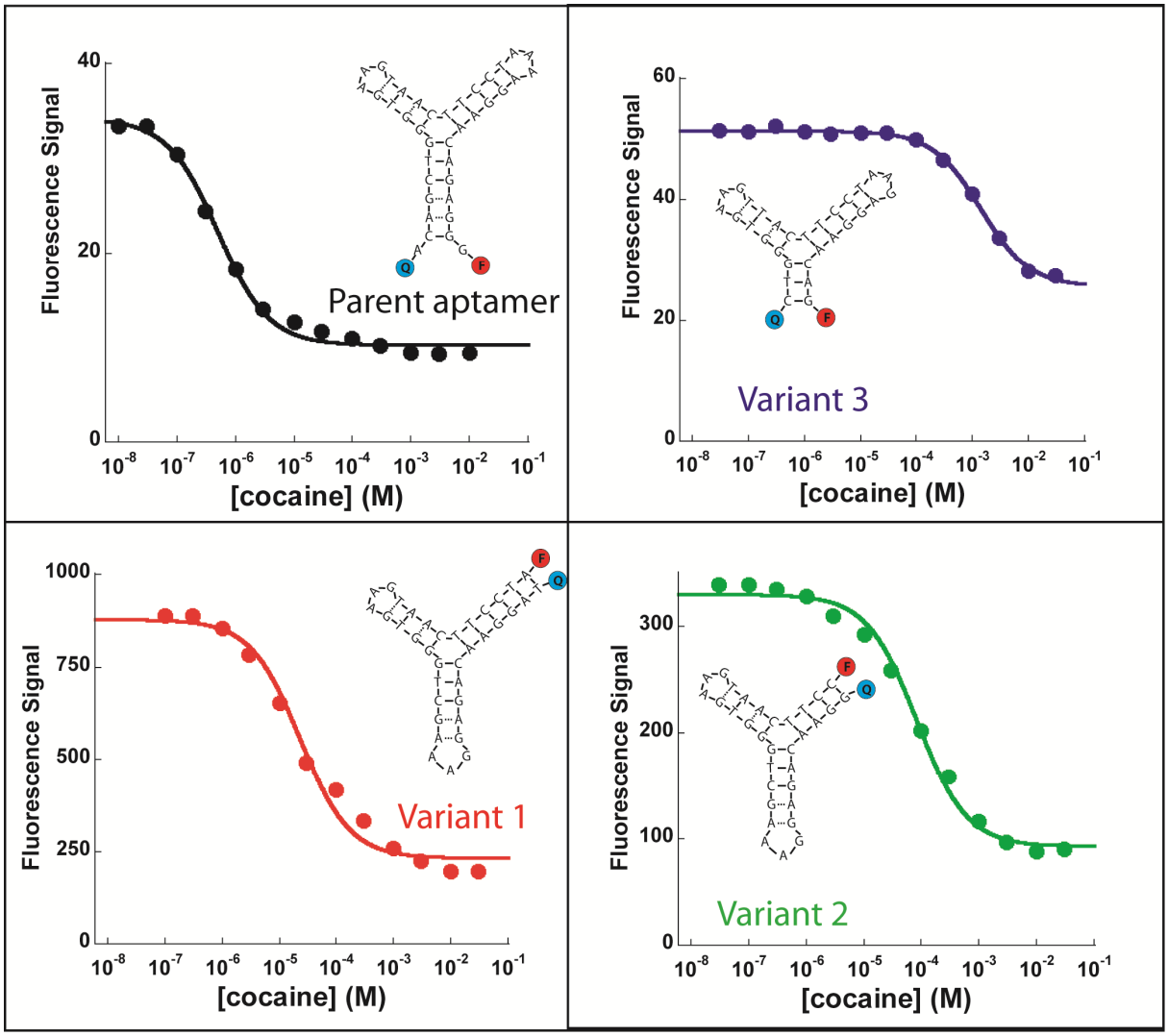

Figure S5: The gain of the four aptamer sequences (parent aptamer + 3 variants) we used to extend and narrow the dynamic range differ significantly.

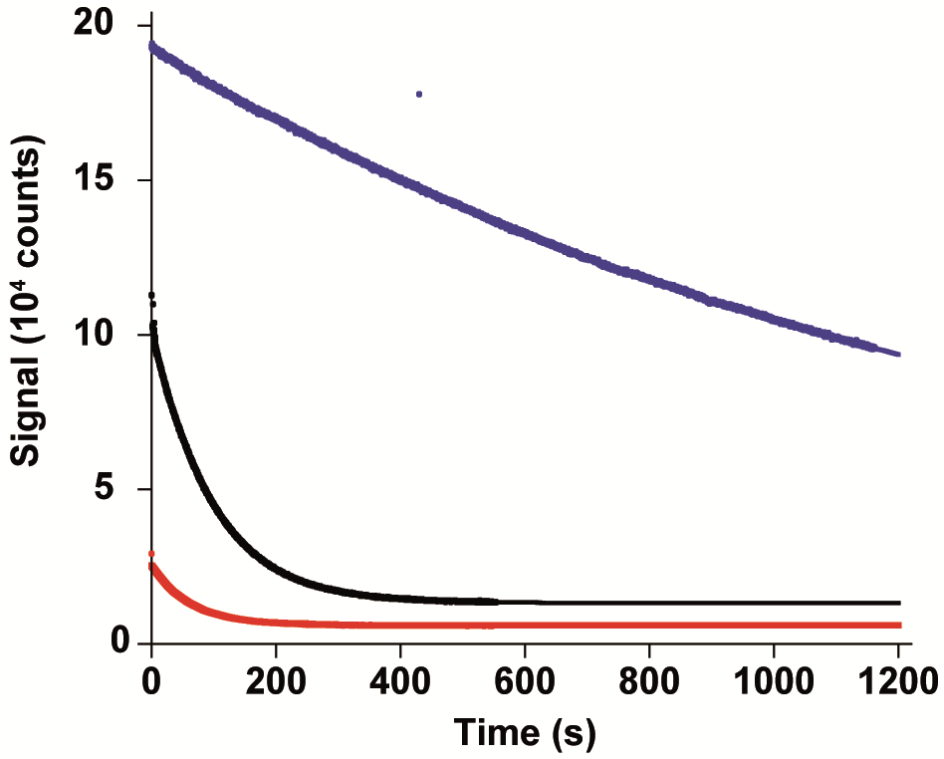

Figure S6: Allosteric inhibitors change the binding kinetic of the aptamer for its target. Shown are the kinetic traces obtained with 100 nM of inhibitor and with 3 mM of cocaine. Inhibitors used are inhibit_10 (10mer inhibitor, red line), inhibit_12 (12mer inhibitor, black line) and inhibit_14 (14mer inhibitor, blue line).